On Stokes Sets

Yuliy Baryshnikov (yuliyb@math.uvsq.fr)
LAMA, Department of Mathematics, Université de Versailles-Saint-Quentine

Abstract. We study combinatorics of Stokes sets appearing in the theory of the asymptotic integral expansions and closely related bifurcation diagrams of quadratic differentials. Hidden within these bifurcation diagrams are Stasheff polyhedra and their relatives.

Introduction

The main goal of these notes is to describe the combinatorial structure of the Stokes sets for the polynomials in 1 variable, a certain bifurcation diagram in the space of monic polynomials of given degree (precise definition is given in section 5). As it turns out, their structure is connected intimately to other bifurcation diagrams (of quadratic differentials, or of Smale functions), and to various combinatorial structures, most prominent of them being Stasheff polyhedra. These notes are expository with proofs at best sketched. Detailed exposition will appear elsewhere.

1. Stasheff polyhedra

1.1. Generalities

Recall some interpretations of the *associahedra*, alias *Stasheff polyhedra*. Denote by B_n the set of all meaningful bracketings of $(n+2)$ indeterminables written in a line (that is the set of ways to form products in a nonassociative algebra).

Join a pair of bracketings by an edge if they are related by one application of the associativity relation, $(a(bc)) = ((ab)c)$. It turns out that the resulting graph is the 1-skeleton of a convex polyhedron whose vertices are the elements of B_n, called the Stasheff polyhedron or the associahedron and denoted by K_n. The faces of K_n are again Stasheff polyhedra and their products.

There are further interpretations of the Stasheff polyhedron (a general reference being, e.g. [15]): it is a geometric realization of the posets of triangulations of a convex plane $(n+3)$-gon or of plane rooted trees with $(n+2)$ leaves. More precisely, an (incomplete) triangulation of a convex polygon is just a collection of nonintersecting chords; ordered by inclusion, these triangulations form a poset dual to the face poset of

K_n. Similarly, assuming that a tree obtained by contracting an edge is greater than the original one, one obtains a partial order on the plane rooted trees isomorphic to the face poset of K_n.

There are several ways to construct convex polyhedra combinatorially equivalent to K_n. We will make use of the following explicit convex polyhedral realization of $K_n \subset \mathbb{R}^n$:

$$K_n(\epsilon) = \{(t_1, \dots, t_n) : |t_i| \le 1, 1 \le i \le n; \sum_{i=j}^{k} t_i \le \epsilon, 1 \le j < k \le n\}.$$

(Here ϵ is a small enough positive number).

More symmetric convex realizations (having the dihedral symmetry) can be obtained using the interpretation of the polyhedron K_n as the fiber polytope of the projection of $(n+2)$ simplex onto the regular polygon with $(n+3)$ vertices [4].

1.2. Stasheff fan

Recall that a fan in a real vector space is a finite stratification of $\mathbb{R}^n$ by convex polyhedral cones C_i such that the relative boundary of any of the cones is a union of the cones of smaller dimensions and the intersection of any two cones is again a cone of the family.

The normal fan associated to a convex compact polyhedron P is defined as the collection of cones $\{C_f\}$ in the dual space, where f runs over faces of P: the cone C_f consists of the linear functionals attaining their maxima over P on f.

Stasheff fan is a fan whose cones ordered by inclusion form a poset dual to that of the facets of K_n, for example, the normal fan to a Stasheff polyhedron (or rather to a convex realization of it, like $K(\epsilon)$, or the symmetric realization).

There is also an explicit construction of a Stasheff fan (related in a natural way to the triangulation interpretation) which we will use further:

Let $\mathbf{P}$ be a convex $(n+3)$-gon in the plane. We call a (real-valued) function on the set of vertices of $\mathbf{P}$ a *balanced weight* if its values add to zero and the geometric center of masses is at the origin (so that the balanced weights form a real vector space of dimension n). A weight is called *degenerate* if there exists a linear function on plane, whose restriction to P majorizes the weight and coincides with it in at least four points.

The partition of $\mathbb{R}^n$ defined by degenerate balanced weights is a Stasheff fan $\Sigma_n \subset \mathbb{R}^n$. The natural stratification of $\mathbb{R}^n$ defined by the Stasheff fan Σ_n is simplicial (in other words, the Stasheff polyhedron

is simple). The number of open simplicial cones in the Stasheff fan of dimension n is $\frac{1}{n+1}\binom{2n}{n}$, that is the Catalan number c_n. The generating function for the Catalan number, $\Phi = \sum c_n t^n$ solves the functional equation

$$\Phi(t) = (1 + t\Phi)^2; \quad \Phi = 1 + 2t + 5t^2 + 14t^3 + \dots.$$

2. Quadratic differentials

2.1. Bifurcation diagrams

Quadratic differentials (a general reference here is [13]), that is differential elements $f(z)dz^2$ with holomorphic f, define a pair of orthogonal (singular) foliations on the Riemann surface V of z as follows: the vectors $\xi \in T_z V$ are tangent to the *horizontal* (*vertical*) foliation iff $f(z)\xi^2 > 0$ ($f(z)\xi^2 < 0$, respectively). The foliations are well-defined everywhere outside the zeros of f; near a zero of order k they have $(k+2)$ rays emanating from the zero.

When the zeros of f are simple, the singularities of each foliation are "tripods" at each zero. For special parameter values special trajectories ("instantons") appear: some of the singular leaves can connect different zeros. This happens on a set of parameters of real codimension 1. The picture below shows a typical behavior of the singular trajectories of a quadratic differential along a 1-parametric transversal to the bifurcation diagram.

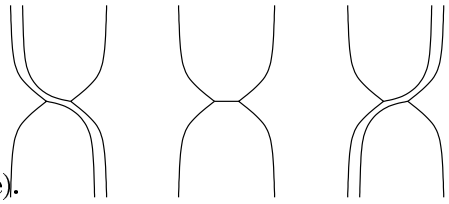

Figure 1. Homoclinic trajectory of a quadratic differential (λY-catastrophe).

DEFINITION 2.1. *Let $\mathcal{L}$ be the base of the versal deformation of a quadratic differential fdz^2. The bifurcation diagram $\mathbf{S} \subset \mathcal{L}$ of the quadratic differential is the closure of the set of parameter values corresponding to quadratic differentials with a singular leaf (horizontal or vertical) joining two zeros of the differential.*

The bifurcation diagram naturally splits into the union of the *vertical* and *horizontal* ones, depending on to which of foliations the nongeneric leaf belongs: $\mathbf{S} = \mathbf{S}_v \cup \mathbf{S}_h$. The bifurcation diagram Δ of zeros of the

quadratic differential, that is the set of parameter values corresponding to differentials with multiple zeros is a subset of $\mathbf{S}_v \cap \mathbf{S}_h$.

The study of the bifurcation diagrams of quadratic differentials was initiated by J. Bruce and D. O'Shea [5] in connection with their investigations of fields of principal directions on minimal surfaces in a 3-dimensional Euclidean space (such surfaces can be invariantly equipped with a conformal structure and a quadratic differential) It seems that the question about the local structure of these bifurcation diagrams has not been investigated earlier (see however [6]).

Below I describe, following [2] the combinatorial structure of the bifurcation diagram in the base of the versal deformation of 'A_n-singularity', that is the quadratic differential $z^{n+1}dz^2$.

The general theory of versal deformations of holomorphic forms fdx^λ was developed by V. Kostov, S. Lando and others (a general reference is [11], see also [9]). In our case of the quadratic differentials (which was already treated in [6]), the base of versal deformation can be identified with the n-dimensional complex linear space of monic polynomials of degree $(n+1)$ with vanishing sum of zeros.

In their preprint Bruce and O'Shea calculated the bifurcation diagram for A_1 case. For the standard deformation $(z^2-a)dz^2$ it consists of two straight lines in the a-plane intersecting at the origin.

2.2. Combinatorics of bifurcation diagrams

Represent $\mathcal{L} = \mathbb{C}^n$ as the product of two $\mathbb{R}^n$'s and consider two cylinders over Σ_n in each of the factors, $\bar{\Sigma}_v = \Sigma_n \times \mathbb{R}^n; \bar{\Sigma}_h = \mathbb{R}^n \times \Sigma_n$.

THEOREM 2.2. *Bifurcation diagram in the base of versal deformation of the quadratic differential $z^{n+1}dz^2$ is homeomorphic to the union $\bar{\Sigma}_v \cup \bar{\Sigma}_h \subset \mathbb{R}^n \times \mathbb{R}^n$, that is there exists a homeomorphism $h : (\bar{\Sigma}_v \cup \bar{\Sigma}_h, \mathbb{R}^m \times \mathbb{R}^m) \to (\mathbf{S}_v \cup \mathbf{S}_h, \Lambda)$ taking $\bar{\Sigma}_h$ to S_h and $\bar{\Sigma}_v$ to S_v .*

In other words, the bifurcation diagram $\mathbf{S}$ is homeomorphic to the fan dual to the *product* of two Stasheff polyhedra.

The number of connected components of the complement to the bifurcation diagram in the base of the versal deformation of A_n-singularity is therefore equal to c_n^2. For example, the cross of Bruce and O'Shea divides $\mathbb{R}^2$ into $4 = 2^2$ pieces.

Consider the *core* $h(\{0\} \times \mathbb{R}^n)$ of the vertical component of the bifurcation diagram (the subset of parameters for which $n-1$ instantons exist). This is a topological submanifold. The intersections of the vertical component $\mathbf{S}_v$ with the germs of transversals to the core are combinatorially Stasheff fans, but their geometry varies strongly. Over

a generic point it is diffeomorphic to the dual fan to the realization $K(\epsilon)$, as on the left part of the Figure 2 below.

On the other hand, the intersection of the vertical component with the core of the horizontal component has the dihedral symmetry, indicated on the right part of the Figure 2.

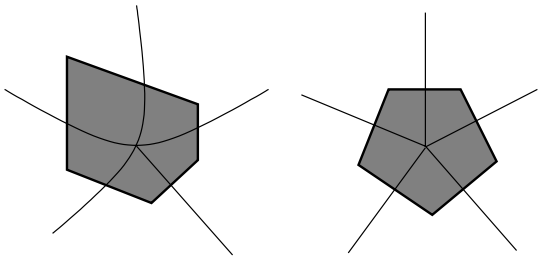

Figure 2. Possible geometries of the intersection of the vertical bifurcation diagram with transversals and their dual Stasheff polygons.

Both components of the bifurcation diagram, S_h and S_v, consist of a large number of pieces of analytic (outside of the discriminant) hypersurfaces. Quite surprisingly, these pieces glue together upon analytical continuation:

THEOREM 2.3. *There exist two hypersurfaces H_v and H_h in $\Lambda \cong \mathbb{R}^{2n}$ which are analytic and irreducible in the complement to the bifurcation diagram of zeros Δ, such that $\mathbf{S}_v \subset H_v$ and $\mathbf{S}_h \subset H_h$.*

The analytic hypersurface from Theorem 2.3 is non-algebraic, unlike the swallowtail. It has a logarithmic branching at Δ.

3. Weighted chord diagrams

3.1. Definitions

To construct the homeomorphism of Theorem 2.2 we will use the description of the Stasheff fan given in 1.2 in terms of balanced weights. The balanced weights give rise to weighted chord diagrams in the plane convex polygon $\mathbf{P}$ with $(n+3)$ vertices.

A *weighted chord diagram* in $\mathbf{P}$ is a set of non-intersecting chords or diagonals (segments joining not neighboring vertices of the convex $(n+3)$-gon $\mathbf{P}$) with a positive number attached to each chord. This set will be called the support of the weighted chord diagram. If the number of chords is maximal (that is, n) we will call the weighted chord diagram *complete*. Complete chord diagrams correspond to triangulations of $\mathbf{P}$.

One can associate a weighted chord diagram to each balanced weight as follows. Fix a point p in the plane of $\mathbf{P}$ which is in general position with respect to vertices of $\mathbf{P}$. Let a balanced weight f be given. For any

two not neighboring vertices of $\mathbf{P}$ consider all linear functions coinciding with f at those vertices and majorizing f elsewhere. The values of these functions at p sweep an interval; its length we take as the weight of the chord joining the vertices. One can check immediately, that the chords with nonzero weight do not intersect and therefore the weight defines a weighted chord diagram.

Conversely, any weighted chord diagram gives rise to a balanced weight.

3.2. Polyhedral model

Balanced weights corresponding to weighted chord diagrams with a given support form a simplicial cone of the dimension equal to the number of chords. Denote this cone by $C_d = \mathbb{R}^D$, where D is a set of nonintersecting chords (i.e. a chord diagram).

Recall that the chord diagrams (without weights) are ordered by inclusion. For any ordered pair of chord diagrams $D_1 \subset D_2$ the cone C_{D_1} is embedded into C_{D_2}: just set the weights of the extra chords to be equal to 0. Gluing all these cones together along these mappings (or, equivalently, taking the inductive limit) one arrives at a "polyhedral model" of $\mathbb{R}^n$ built of simplicial cones corresponding to chords diagrams. The cones of the Stasheff fan of positive codimension correspond to the images of the cones $C_d, |D| < n$.

4. Quadratic differentials and weighted triangulations

4.1. From quadratic differentials to weighted chord diagrams

According to [11], the standard affine deformation

$$f(z;a)dz^2 = (z^{n+1} + a_1 z^{n-1} + \ldots + a_n)dz^2$$

of the A_n singularity of quadratic differential is versal. Now we associate a pair of weighted chord diagram to each value of parameter $a = (a_1, \ldots, a_n)$.

For each a one can choose $R > 0$ large enough, so that outside of the circle $C_R = \{|z| \leq R\}$ the fields of directions defining any of the foliations is sufficiently close to the fields of directions corresponding to the unperturbed differential $z^{n+1}dz^2$. In particular, the union of leaves of (say) the horizontal foliation intersecting C_R consists of $(m+3)$ arms going to infinity. We identify once and forever these arms with the vertices of the convex polygon $\mathbf{P}$.

Take R so large that the interior of C_R contains the set Z of zeros of f. We will call a nonsingular horizontal leaf *nontrivial*, if its intersection with C_R represents a nontrivial element of $\pi_1(C_R - Z, \partial C_R)$. A connected component of the union of nontrivial leaves we will call a *stream*. Apparently, a stream goes from infinity to infinity along two different arms. The integral of (a branch of) the 1-form $\sqrt{f}dz$ sends the stream to an infinite horizontal strip on the complex plane. The height of this strip we call the *weight of the stream*. Join the vertices of **P** corresponding to the arms containing the stream by the chord and attach to it the weight of the stream. What results is a weighted chord diagram. The same can be done with the vertical foliation.

Therefore, one can associate a pair of weighted chord diagrams corresponding to the horizontal and vertical foliations to each (deformed) quadratic differential fdz^2 (see an example on Figure 3 below).

4.2. ...AND BACK

This correspondence can be inverted: for each pair of weighted chord diagrams, there exists unique (given that the sum of its zeros vanishes) polynomial quadratic differential which generates exactly them.

For example, if both chord diagrams are empty (that is, the weights of all chords are zeros), we arrive at polynomial z^{n+1}.

To describe the inversion, it will be convenient to draw two polygons (with $(n+3)$ vertices each) in which the chord diagrams in question are given as inscribed with alternating vertices into a $2(n+3)$-gon **D**. We will call this configuration the *interlacing* polygons. This reflects the behavior of the arms of the horizontal and vertical foliations at infinity.

Let the chords with positive weights be represented by straight segments joining the vertices of the large polygon. They divide the interior of the polygon into several connected components. We put one point into each of the components and join these points by segments if the corresponding components share a segment of a chord on their boundaries. Further, we join the interior point in each component with the vertices of **D** which belong to the boundary of the component.

These segments divide the polygon **D** into convex polygons of the following types:

a) triangles with one side being a side of **D**;

b) triangles with exactly one vertex being a vertex of **D**. Such a triangle has to contain a piece of exactly one chord.

c) 4-gons containing exactly one point of intersection of chords (one vertical and one horizontal). All the vertices of the 4-gon are interior points of **D**.

Replace each triangle of type a) by the quarterplane; each triangle of type b) by the half-infinite rectangular strip of width equal the weight of the chord piece of which the rectangle contains; and each 4-gon by a rectangle whose sides are equal to the weights of the chords intersecting inside the component. One can identify the corresponding sides of the boundaries of these new geometric pieces.

The resulting (topological) disk acquires the conformal structure, which is flat everywhere outside of $(m+1)$ internal points where more than four right angles of the flat pieces come together. We will denote these points by p_i. There exists unique complex structure compatible with the conformal one. As is easy to check, the disk is conformally equivalent to the entire complex plane $\mathbb{C}$. Choose a coordinate z on this plane so that the sum of coordinates of p_i's vanishes, and the directions to the images of the vertices of $\mathbf{D}$ are positioned correctly (remember that they are identified with the arms of a polynomial quadratic differential, which tend asymptotically to directions $\exp(i\pi k/(n+3)), k = 0, \ldots, 2n+3$). This fixes the coordinate z. Let the coordinates of the points p_i be z_i, $i = 1, \ldots, n+1$ (counted with multiplicities), and take f to be the monic polynomial of degree $m+1$ with roots z_i. Then the polynomial quadratic differential $f(z)dz^2$ generates the pair of weighted chord diagrams we have started with. *This proves Theorem 2.2.*

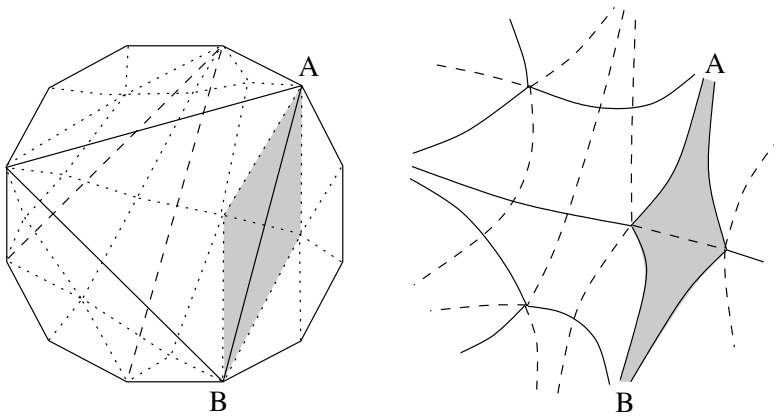

Figure 3

A pair of chord diagrams and the foliations defined by the corresponding polynomial quadratic differential of degree 4 are shown on Figure 3. Here the solid diagonals on the left picture and the solid lines on the right picture correspond to vertical foliation; dashed diagonals and dashed lines to the horizontal one. The auxiliary segments subdi-

viding $\mathbf{D}$ are shown as dotted. The pieces corresponding to the diagonal AB and the corresponding stream are filled.

The linear space of monic polynomials with vanishing zero sum can be identified not only with the base space of the versal deformation of quadratic differential $z^{n+1}dz^2$ but also with the base space of the versal deformation of the simple singularity A_n of *plane curves* [1]:

$$a \mapsto P_a(z,w) = f(z,a) - w^2, \text{ where } f(z,a) = z^{n+1} + a_1 z^{n-1} + \ldots + a_n.$$

The discriminant Σ is the set of values of parameters a for which the level curve $X_a = \{(z,w) : P_a(z,w) = 0\}$ is singular (equivalently, for which $f(\cdot,a)$ has multiple roots). Let $\omega = wdz$. This holomorphic 1-form ω defines a section of the cohomological Milnor fibration over $\Lambda - \Delta$ (the fibers of this fibration are $H^1(X_a, \mathbb{C})$) defined by the restrictions of ω to X_a. The integral of the form over a locally constant (with respect to the Gauss-Manin connection) section of the homological Milnor fibration defines a (multi-valued) holomorphic function on $\Lambda - \Delta$. For a cycle constructed from a vertical (horizontal) instanton the real (imaginary) part of this function vanishes. This shows that each of the two components of the bifurcation diagram, S_h and S_v, are analytic real hypersurfaces in $\Lambda \cong \mathbb{R}^{2m}$.

For example, for the standard deformation of the Morse singularity A_1,

$$f(z,a) = z^2 - a,$$

we have $h = a$ (up to a multiplicative constant), and the cross of Bruce and O'Shea is just the union of lines $\Re(a) = 0$; $\Im(a) = 0$.

Consider the base space $\mathcal{L}$ as just the real linear space and let $\mathcal{L}^{\mathbf{D}}$ be its complexification (that is $\Lambda^{\mathbf{D}} \cong \Lambda \otimes_{\mathbb{R}} \mathbb{C}$). The function $\Re(h)$ locally defining the bifurcation diagram of quadratic differential near a smooth point is locally holomorphic and its zero locus is an analytic hypersurface. This hypersurface is singular and non-algebraic (the function h has logarithmic terms near Δ).

The discriminant Δ extends to $\Lambda^{\mathbf{D}}$ as an algebraic singular variety of (complex) codimension 2. In Example 4.2 ???? the discriminant is just the origin in the plane. Both strata of the bifurcation diagram are smooth at the origin. Generally, both S_v and S_h are smooth at the smooth points of Δ. Indeed, let $a_0 \in \Sigma \in \Lambda^{\mathbf{D}}$ be a generic point of the discriminant, such that only two zeros of p_{a_0} coincide and there is no nontrivial instanton trajectories. In a neighborhood of a_0 we consider the set $\mathbf{S}_{v;a_0}$ consisting of quadratic differentials with a vertical trajectory connecting the colliding at a roots of p_a. Clearly, the hypersurface $\mathbf{S}_{v;a}$ is smooth at a.

The union of hypersurfaces $\mathbf{S}_{v,\Delta} = \cap_{a\in\Delta} S\_v; a$ is smooth irreducible (as Δ is irreducible) hypersurface in a tubular (of varying radius) neighborhood of Δ in $\Lambda^{\mathbf{D}}$.

If a_0 is a generic point of the bifurcation diagram $\mathbf{S}_v$, the path constructed in the beginning of this Section belongs to the smooth part of the diagram and connects a_0 to $\mathbf{S}_{v,\Delta}$. The irreducibility of $\mathbf{S}_{v,\Delta}$ implies Theorem 2.3.

5. Stokes sets

5.1. Stokes phenomena

The motivation for the study of Stokes sets comes primarily from the theory of asymptotic expansions of integrals using the steepest descent method.

Consider the approximation of the integrals

$$I(k;l) = \int_C a(x;l)e^{k\Phi(x;l)}dx$$

for $k \to \infty$. Here the phase Φ is an analytic in $\mathbb{C}$ function depending analytically on some parameters l and C is an infinite contour such that $\Re\Phi \to -\infty$ at its ends (that is C represents some element of $H_1(\mathbb{C}, \{\Re\Phi \ll 0\})$). To approximate this integral one customarily deforms the contour to pass through the critical points of Φ and to go along the trajectory of the steepest descent (that is the trajectory of the gradient vector field of the real part of Φ). These trajectories are the leaves of the foliation defined by the level curves of the imaginary part of Φ. The nighborhoods of the critical points of the phase contribute most to the integral.

The form of the asymptotic expansion thus obtained depends on number of critical points through which the steepest descent contour passes. Typically, one has

$$I(k;l) = m_1 e^{k\Phi(x_1(l))} + m_2 e^{k\Phi(x_2(l))} + \dots,$$

where x_i are the critical points of Φ on the deformed contour; m_i are some functions of k and l slowly (as compared to the exponential function) varying with k. The main contribution comes, of course, from the critical values with the largest real part.

The Stokes phenomenon in this context is the discontinuous change of the coefficients m (Stokes' multipliers) as the parameters l change. The topological reasons for this is the discontinuous behavior of the gradient trajectories at the parameter values when a segment of the

trajectory connects two critical points. This is a nongeneric situation which happens in real codimension 1. A typical example is shown below.

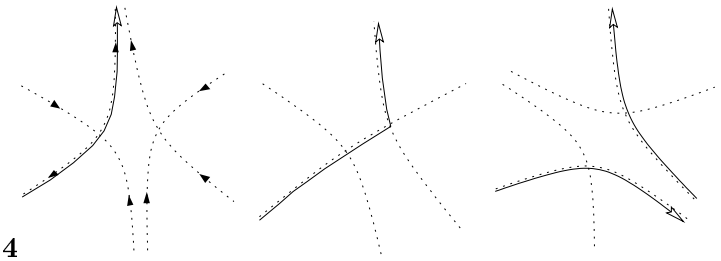

Figure 4

Here the contour is shown as a solid line; dotted lines show the foliation by the level lines of the imaginary part of the phase.

Notice that at the bifurcation set, the real parts of the critical values are strictly different: the Stokes phenomenon does *not* reduce to one critical value bypassing the other and becoming the leading exponent. A subset of parameters where this happens (antiStokes sets, see below) is also relevant in asymptotic analysis and in our constructions.

At the bifurcation set the imaginary parts of the critical values connected by the gradient trajectory coincide. However, the Maxwell stratum for the imaginary part of Φ is strictly larger than the set of parameters where the Stokes phenomenon occurs: the existence of the connecting gradient trajectory is necessary. The Maxwell strata for the imaginary parts of holomorphic germs were studied in [10].

5.2. Stokes sets

The Stokes set associated with an asymptotic integral depends on the class of integration contour; taking into account all possible contours, we get the following definition.

DEFINITION 5.1. *Let $\Phi : U \times \mathcal{L} \to \mathbb{C}, U \subset \mathbb{C}, \mathcal{L} \cong \mathbb{C}^m$ be a deformation of the function $\phi(\cdot) = \Phi(\cdot; 0), l \in \mathcal{L}$. The Stokes set $\mathbf{S}_v \subset \mathcal{L}$ is the closure of the set of parameters for which there exists a smooth component of a level set of the imaginary part of $\Phi(\cdot, l)$ with critical points at its ends.*

Similarly, the antiStokes set $\mathbf{S}_h \subset \mathcal{L}$ is defined in terms of the foliation by the level curves of the real part of Φ.

The bifurcation diagram of functions $\mathbf{D}$ is apparently a stratum in $\mathbf{S}_v \cap \mathbf{S}_h$.

Example. The Stokes set for the Airy function (corresponding to $\Phi(x, l) = x^3/3 + xl, l \in \mathbb{C}$) is the union of three rays from the origin at 120°; the antiStokes set is the centrally symmetric image of the Stokes set.

6. Even polygons and quadrillages

For multiparametric deformations these elementary Stokes sets, in words of M. Berry, "coalesce or cross". He says further that "there ought to be a classification of the ways in which this can happen stably..." [3]. A description of the combinatorics of the Stokes and antiStokes sets follows.

6.1. Definitions

We will again use the polygons in a fashion similar to that of section 4.

All polygons we will consider here will be assumed "marked" meaning that their vertices are numbered from 1 through v counterclockwise. We will call a convex polygon with an even number of vertices simply an *even polygon*.

DEFINITION 6.1. *A quadrillage of an even polygon P is a set of non-intersecting chords which partition P into even polygons. The number of chords is called the size of a quadrillage. A quadrillage of maximal size (that is such that all polygons of the partition are 4-gons) is called complete.*

Complete quadrillages of marked even polygons correspond to rooted ternary trees just as triangulations correspond to rooted binary trees. The generating functions

$$Q(t) = \sum_0 q_n t^n$$

where $q_n = \#\{\text{complete quadrillages of } 2n+2\text{-gon}\}t^n$ solves the functional equation

$$Q = (1 + tQ)^3$$

(the analogous equation for triangulations with squared, not cubed, term, leads to the Catalan numbers) and implies, via Lagrange inversion, $q_n = \frac{1}{2n+1}\binom{3n}{n}$; $\Phi = 1 + 3t + 12t^2 + 55t^3 + 273t^4 + \ldots$.

For each even polygon we fix one of the two interlacing assignments of signs $(+)$ and $(-)$ to its vertices; the even polygon with such an assignment is called *signed*. For signed polygons one obtains an orientation of the chords of a quadrillage and of the sides of the polygon $\mathbf{P}$: each of them is oriented from a $(-)$ towards a $(+)$.

An (ordered) pair of *interlacing* polygons (having the same number of vertices v) is a convex polygon $\mathbf{D}$ with $2v$ vertices $1, 2, \ldots, 2v$ numbered counterclockwise; the even vertices thought of as the vertices of one polygon; the odd ones as the vertices of the other.

We consider two interlacing *even, signed* polygons $\mathbf{P}_v$ and $\mathbf{P}_h$ called respectively vertical and horizontal, and their quadrillages (also called vertical and horizontal). Fix the first vertex of $\mathbf{D}$ to be horizontal and the first two vertices to be (+)-signed. This sign assignmenet induces an orientations (as described above) on the chords and sides in each of the interlacing even polygons.

DEFINITION 6.2. *Two quadrillages of a pair of interlacing even polygons P_h and P_v is called admissible if for any couple of intersecting chords c_h and c_v of the respective polygons, the sense of the orientation at the intersection point defined by the tangent vectors to c_h and c_v (in this order) is positive.*

Notice that the orientations at the intersections of chords and *sides* of the polygons are automatically positive, due to the chosen numbering/signing scheme.

For example, of the 3×3 pairs of complete quadrillages of interlacing 6-gons, 6 are admissible and 3 are not, see the figure below.

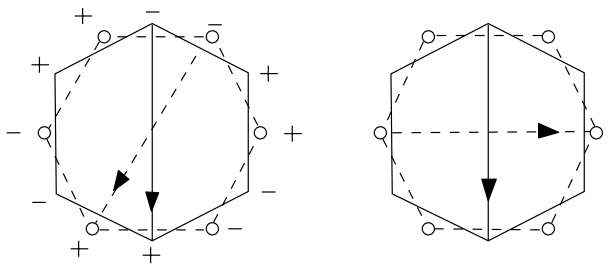

Figure 5. The dashed chords are horizontal; the solid ones — vertical.

6.2. Combinatorics of Stokes/antiStokes sets

Similarly to 3.2, we associate to each admissible pair of quadrillages $\pi = (q_v, q_h)$ the simplicial cone C_π of the nonnegative weights on its chords. The dimension of this cone is clearly the sum of the sizes of the quadrillages.

The pairs of quadrillages are ordered by inclusion (as the quadrillages themselves are). For any two ordered admissible pairs of quadrillages $\pi_1 = (q_v^1, q_h^1) \prec \pi^2$ we denote by $i_{\pi_1\pi_2} : C_{\pi_1} \to C_{\pi_2}$ the embedding attaching zero weights to the missing chords.

Gluing the cones C_π together using these embeddings we arrive at a simplicial complex (or rather a cone over a simplicial complex) which we denote by Λ.

The union of the (images of) the cones with noncomplete vertical quadrillages will be denoted by Σ_v; the same for the horizontal quadrillages will be denoted Σ_h. Clearly, Σ_v and Σ_h are simplicial subcomplexes of Λ.

Consider also the admissible pairs of noncomplete quadrillages which have the property that they can be augmented by a pair of intersecting (one vertical, one horizontal) chords. The (image of the) union of the corresponding cones we denote by Σ.

The relevance of all these combinatorial constructions to our problem is explained by the following result.

THEOREM 6.3. *There exists a homeomorphism of quadruples*

$$w : (L; S_v, S_h; S) \to (\Lambda; \Sigma_v, \Sigma_h; \Sigma)$$

which is a diffeomorphism outside of S.

In particular, the space Λ is a cone over a sphere. The connectedness of the sphere implies, in particular, that any two complete quadrillages can be connected by a sequence of elementary flips (removing a chord and replacing it by another one in the resulting hexagon).

This result is entirely analogous to Theorem A: to construct w one just considers the quadratic differential $(f_p' dz)^2$ and applies the gluing method. The only condition to check is that the resulting partitions of the interlacing polygons satisfy the conditions of the theorem and, conversely, that any admissible pair of weighted quadrillages gives rise to a quadratic differential on $\mathbb{C}$ with even zeros only.

The analogue of Theorem 2.3 is also valid:

THEOREM 6.4. *For* $n \geq 3$ *the union of the Stokes and antiStokes sets belongs to an irreducible (real) hypersurface in* $\mathcal{L}$ *(considered as a real affine space), analytic outside of the discriminant.*

(The configuration of the Stokes and antiStokes sets for the Airy function shows that both of them belong to the same irreducible hypersurface).

The connected components of $\Lambda - \Sigma_v$ are numbered by complete quadrillages of the v-gon with ordered vertices.

PROPOSITION 6.5. *The connected components of* $\Lambda - \Sigma_v$ *are cells.*

7. Polyminos

Fix a quadrillage q subdividing the $2n+2$-gon into n 4-gons. It will be convenient to think of the quadrillage as of a *polymino* (e.g., a hexagon with 1 large diagonal correspnds to the doino).

An n-polymino is defined as following. Consider a collection $\mathbf{S}$ of n copies of the unit square in the plane $\{|x| \leq 1/2, |y| \leq 1/2\}$ (thus equipped with an orientation). The sides of these squares are oriented by the condition that together with the outward normal they form a positive frame. A polymino is the space resulting from the identifications of several sides of the squares in such a way that

a) the orientations of the identified sides are opposite if one of them is vertical and one is horizontal and the same otherwise;

b) any two squares have at most 1 side identified and

c) the resulting space is connected.

More formally, let $\mathbb{S}$ be the set of sides of the squares in $\mathbf{S}$. Consider a partition of $\mathbb{S}$ into a family of subsets denoted by $\mathbb{E}$; the element to which the side α belongs is denoted by $e(\alpha)$. The partition of $\mathbb{S}$ into the sides belonging to the same square we will encode via the function $s : \mathbb{S} \to \mathbf{S}$; $s(\alpha)$ is therefore the square of which α is a side.

Further, take a family of isometries $\phi_\alpha : S_\alpha \to \mathbb{R}$, where α runs through $\mathbb{S}$, which *preserve orientations* when α is a horizontal edge and *reverse it* if it is a vertical one, and send the midpoints of the edges to zero. Now, we identify the points of the edge with the same $e(\alpha)$ having equal values of ϕ_α. The resulting cell complex is called a *polymino* $\mathbf{p}$.

We will assume (without loss of generality, to exclude some trivial cases) that each subset of the partition $\mathbb{E}$ with more than 1 element contains both vertical and horizontal sides.

The *backbone* of the polymino is the graph whose vertices are the centers of the squares (these elements will be called s-vertices) and of their *identified* edges, that is of points numbered by elements of $\mathbb{E}$ (called e-vertices). The edges of the backbone are numbered by the elements of $\mathbb{S}$ and the edge α connects the s-vertex $s(\alpha)$ with the e-vertex $e(\alpha)$.

The backbone graph is clearly bipartite (into e- and s-vertices) and naturally oriented: an edge α points from an s-vertex towards an e-vertex if α is vertical and in the oposite direction if α is horizontal.

A polymino is called *ordered* if this orientation of the backbone graph has no cycles.

We say that a polymino is *simple* if any side of any square is identified with at most one side of some other square. Examples of nonsimple and unordered polyminos are given on the figure below.

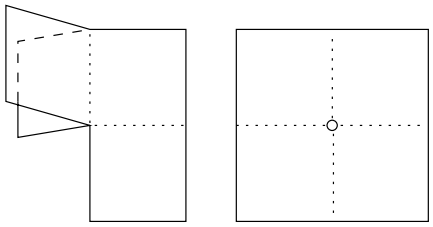

Figure 6. Nonsimple (left) and unordered (right) polyminos.

Denote by $V(\mathbf{p}) = \mathbb{R}^{\mathbb{S}(\mathbf{p})}$ the real vector space of functions on the edges of the backbone. The projection sending an edge to its e-vertex embeds the space $E(\mathbf{p}) = \mathbb{R}^{\mathbb{E}}$ of functions on e-vertices into $V(\mathbf{p})$.

To each polymino $\mathbf{p}$ we associate a fan $\mathbf{S}(\mathbf{p})$ in the real vector space $V(\mathbf{p})/E(\mathbf{p})$. To define a fan it is sufficient to define its intersection with a vicinity of the origin. An element of $V(\mathbf{p})/E(\mathbf{p})$ can be identified with the functions w of flags having the property that $\sum_{\alpha \in e} w(\alpha) = 0$ for any E-vertex e.

Provide each unit square of the polymino with the piecewise linear foliation by the level sets of the function

$$|x - 1/2| - |y - 1/2|,$$

Now perturb the isometries ϕ_α defining the polymino as

$$\phi_\alpha \mapsto \phi_\alpha + w(\alpha).$$

Gluing together the squares according to thus modified isometries we obtain (for small w) again a topological space with an oriented foliation.

We say that the vector w is *degenerate* if there exists a trajectory (a piecewise linear immersion of the oriented segment into the polymino tangent to the foliation at all points of linearity) of this foliation and connecting centers of some two squares.

Degenerate vectors form a germ of the associated fan in $V(\mathbf{p})/E(\mathbf{p})$ which we will denote as $\mathbf{S}(\mathbf{p})$.

The relevance of the fans associated to polyminos is that they describe the local combinatorics of the Stokes sets.

PROPOSITION 7.1. *Let $C(\mathbf{p})$ be the cell in the complement to the antiStokes set corresponding to a polymino $\mathbf{p}$. Then there exists a homeomorphism*

$$h : (C(\mathbf{p}), C(\mathbf{p}) \cap \mathbf{S}_v) \to (\mathbb{R}^n, \mathbf{S}(\mathbf{p})) \times \mathbb{R}^n.$$

8. Stokes polyhedra

It turns out that the fans $\mathbf{S}(\mathbf{p})$ for ordered polyminos are dual to certain finite convex polyhedra. We formulate the theorems in terms of polymino, so that they are valid also for those of them not coming from quadrillages of even polygons.

THEOREM-PROPOSITION 8.1. *For every ordered polymino* $\mathbf{p}$*, the fan* $\mathbf{S}(\mathbf{p})$ *is dual to a convex polyhedron* $St(\mathbf{p})$ *called the Stokes polyhedron of* $\mathbf{p}$*.*

The Stokes polyhedra form a family of polyhedra interpolating between the the Stasheff polyhedron and the cube. The examples of Stokes polyhedra for polyminos with at most 4 squares are given below.

More generally, call the *height* of the polymino the length of the longest oriented chain in its backbone graph.

If the height of p is 2, then $St(\mathbf{p})$ is a cube. If the backbone graph itself is a chain, then $St(\mathbf{p})$ is a Stasheff polyhedron. More generally, one has the following result:

PROPOSITION 8.2. *Each Stokes polyhedron of an ordered polymino is a Minkovsky sum of the Stasheff polyhedra corresponding to maximal chains in the backbone graph.*

The Minkovsky summands of some of the 3-dimensional Stokes polyhedra shown on Figure 7 are shaded.

Some further useful properties of the Stokes polyhedra.

PROPOSITION 8.3. *The polymino is simple if and only if the Stokes polyhedron is simple.*

If an s-vertex σ of the backbone graph of $\mathbf{p}$ is *separating* (that is all adjacent edges are either all *in*- or all *out*-vertices), or, equivalently, the square is glued to along only vertical or only horizontal sides, then $St(\mathbf{p})$ is the product of Stokes polyhedra corresponding to the polyminos obtained by removing the square σ and replacing it by its copy in each of the connected polymino into which $\mathbf{p}$ splits upon this removal.

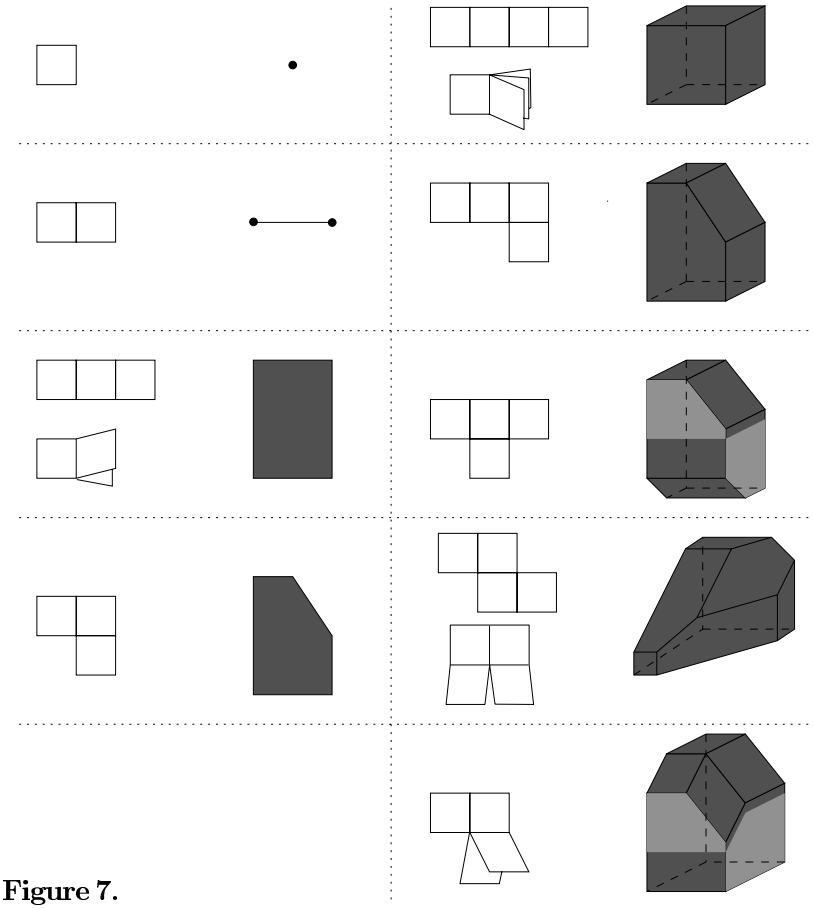

Figure 7.

9. Miscellaneous remarks

9.1. Combinatorics

The Stokes polyhedra have some obvious combinatorial interpretations in terms of enumerations of restricted triangulations (or bracketings). For example, the vertices of the the Stokes polyhedron for the T-shaped tetramino enumerate the triangulations of a heptagon with exactly one of the chords $\mathbf{1-4}$ and $\mathbf{1-5}$ in it.

Enumerating these restricted triangulations allows one to quantify the clam made above that the Stokes polyhedra intrpolate between the (most complicated) Stasheff polyhedron and (least comlpicated) cube.

The number of vertices of the Stokes polyhedron corresponding to the A-type polymino (left on the Figure 8) is the Catalan number c_n ; the number of vertices of the D-type polymono (right one) is $c_n - c_{n-2}$ (both with $(n+2)$ squares).

Figure 8.

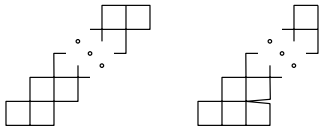

9.2. Singularities

There are some natural ramifications of the theory sketched above (to be described elsewhere). Thus, (ordered) non-simply connected polymino appear naturally in the polyhedral models of the Stokes sets in versal deformations of other singularities.

One can also study the real case (most interting for the applications). All the constructions remain valid; the condition of reality of the deformation just implies that the pairs of the quadrillages and the corrsponding polyminos have an axis of symmetry.

9.3. K-theory

More surprisingly, Stokes polyhedra appear in algebraic K-theory.

Recall that the Steinberg group of order n over a ring R is the free group with generators $x_{ij}^a, 1 \leq i \neq j \leq n, a \in R$ satisfying the relations

$$x_{ij}^a x_{ij}^b = x_{ij}^{a+b}, \qquad \textbf{(A)}$$

$$[x_{ij}^a, x_{kl}^b] = 0 \text{ if } i \neq l \text{ and} j \neq k, \qquad \textbf{(B)}$$

and

$$[x_{ij}^a, x_{jk}^b] = x_{ik}^{ab}, i, j, k \text{ distinct.} \qquad \textbf{(C)}$$

Kapranov and Saito undertook in [8] a study of these relations syzygies between them in a geometric way, the first step of which is to represent the generators of a group as 1-simplices and the relations as 2-cells spanning them, so that the group itself appears as the fundamental group of the resulting cell complex. The next steps then would consist in finding the syzygies between the relations (corresponding to 3-cells), syzygies between syzygies and so on. One can see immediately that the Steinberg relations themselves can be represented as a triangle (relation A), square (relation B) and the pentagon (relation C).

The topology of space obtained by gluing the cells representing the higher syzygies encodes, conjecturally, the higher K-theories.

The first steps of this program has been successfully realized: a family of polyhedra representing the syzygies between Steinberg relations has been proposed in [8], such that the second homotopy group of the resulting CW-complex is equal to $K_3(R)$.

The surprising fact is that all these polyhedra (with exception of those containing a triangle corresponding to the additive relation A) turned out to be the Stokes polyhedra listed in the right column of Figure 7.

An explanation of this comes from the Hatcher-Wagoner approach to K-theory [7].

Recall that a Smale-Morse function is a Morse function such that the stable and unstable manifolds $C^{\pm}(f,x)$ of the gradient flow corresponding to critical points x (that is unions of gradient trajectories of f approaching x as $t \to \pm\infty$) intersect transversally. (Of course this is a property of the pair [function, metric], or rather of the pair [function, gradient-like vector-field], not of the function per se). The unstable manifold $S^{-}(f,x)$ for a Morse-Smale function is diffeomorphic to the Euclidean space of dimension equal to the index of x.

Consider a smooth manifold M^m (with boundary) and a Morse-Smale function f having only Morse critical points of the same index $1 < i < m$ such that

a) all critical values are positive, and

b) the intersections of the unstable manifolds with $\{f = 0\}$ are spheres.

Then, provided with orientations, these unstable manifolds form a basis of $H_i(M, \{f \leq 0\}; \mathbb{Z})$.

Consider now the space $\mathcal{M}$ of Morse functions on M having r critical points and such that the two conditions above are satisfied. For a generic function, the stable and unstable manifolds of different critical points do not intersect, but for some of them this Smale condition is violated. Denote this bifurcation diagram Σ. A result of [7] states that under some dimensional conditions there exists an isomorphism of the Steinberg group with r generators over $R = \mathbb{Z}(\pi_1(M))$ and $\pi_1(\mathcal{M}, \mathcal{M} - \Sigma)$.

A smooth point of the codimension 1 stratum of the bifurcation diagram corresponds to the transversal intersection of the stable and unstable manifolds $S^{-}(f,x)$ and $S^{+}(f,x)$ of some 2 critical points x and y along a gradient trajectory from y to x.

The element of this group represented by a generic 1-parameter deformation passing through a point on the codimension 1 stratum of Σ yields the change of the basis of H_i by an elementary operation.

The codimension 2 strata are either the selfintersections of the smooth parts of codimension 1 strata corresponding to pairs of disjoint trajectories connecting two pairs of critical points, or strata corresponding to chains of three critical points $x \to y \to z$ connected by the gradient trajectories. The former strata correspond to the squares, or, algebraically, to the 4-term relation B; the latter to the pentagon, that is to the 5-term relation C.

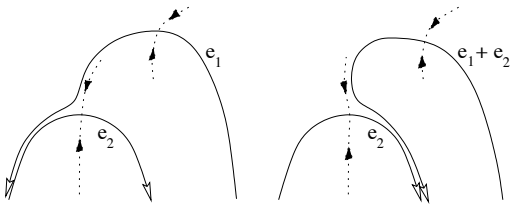

Figure 9. Changes of the homology basis associated with the crossing of the bifurcation diagram

More generally, for any partial order on the set of critical vertices, one can consider the strata consisting of such a Morse function that the ordered points correspond to the critical values connected by a chain of gradient trajectories. One can show that at generic points the CW-complexes dual to this stratification again have combinatorial type of certain convex polyhedra which are Minkovski sums of Stasheff polyhedra.

The bifurcation diagrams associated with polyminos described in Section 7 are obviously a special case of this construction. Moreover, in small codimensions (below 5) bifurcations coming from polymino exhaust the combinatorial types of these polyhedra. This explains their appearance in our lists.

References

1. Arnold, V., Varchenko, A., Gussein-Zade, S. *Singularities of Differentiable Mappings, vol. 2,* Birkhäuser, Boston, 1988.
2. Baryshnikov, Yu. Bifurcation diagrams of quadratic differentials, *C. R. Acad. Sci. Paris*, **325**, 71-76, 1997.
3. Berry, M. Stokes' phenomenon: smoothing a Victorian discontinuity, *Publ. Math. IHES*, **68**, 211-221, 1989.
4. Billera, L.J; Sturmfels, B., Fiber polytopes, *Ann. Math.*, **135**, 527-549, 1992.
5. Bruce, J.W.; O'Shea, D.B., On Binary Differential Equations and Minimal Surfaces, *Preprint*, Liverpool, 1995.
6. Hubbard, J., Masur, H. Quadratic Differentials and Foliations, *Acta Mathematica*, **142**, 1979.
7. Hatcher, A., Wagoner, J.*Pseudo-isotopies of compact manifolds.* Asterisque, No. 6. Societe Mathematique de France, Paris, 1973.
8. Kapranov, M., Saito M., Hidden Stasheff polytopes in algebraic K-theory and in the space of Morse functions, Contemp. Math., **227**, 1998.

9. Kostov, V. P., Versal deformations of differential forms of real degree on the real line, *Math. USSR, Izv.* **37**, No. 3, 525-537, 1991.
10. Kostov, V. P., On the stratification and singularities of the Stokes hypersurface of one- and two-parameter families of polynomials. In: *Theory of singularities and its applications, (V. I. Arnol'd, Ed.)*, **Adv. Soviet Math., 1**, AMS, Providence, 1990, pp. 251–271.
11. Kostov, V. P.; Lando, S. K.; 1993, Versal deformations of powers of volume forms. *Computational algebraic geometry (Nice, 1992)*, **Progr. Math., 109**, Birkhäuser Boston, Boston, MA, 1993, pp. 143-162.
12. Shnider, S., Sternberg, S. *Quantum groups*. Graduate Texts in Mathematical Physics, II. International Press, Cambridge, MA, 1993.
13. Strebel, K. *Quadratic Differentials*, Springer, Berlin, 1984.
14. Wright, F.J. The Stokes set of the cusp diffraction catastrophe, *J. Phys.* **A13**, 2913-2928, 1980.
15. Ziegler, M. *Polytopes*, Springer, Berlin, 199?.

Address for Offprints: 45 Av. des États-Unis, Bât. Fermat, 78035 Versailles, France